



WILEY

ORIGINAL ARTICLE

Anti-inflammation effects of injectable platelet-rich fibrin via macrophages and dendritic cells

Jinglun Zhang^{1,2} | Chengcheng Yin^{1,2} | Qin Zhao^{1,2} | Zifan Zhao^{1,2} |
Jinyang Wang^{1,2} | Richard J. Miron^{3,4,5} | Yufeng Zhang^{1,2}

¹The State Key Laboratory Breeding Base of Basic Science of Stomatology (Hubei-MOST) and Key Laboratory of Oral Biomedicine Ministry of Education, School and Hospital of Stomatology, Wuhan University, Wuhan, China

²Department of Oral Implantology, School and Hospital of Stomatology, Wuhan University, Wuhan, China

³Centre for Collaborative Research, Nova Southeastern University, Cell Therapy Institute, Fort Lauderdale, Florida

⁴Department of Periodontology, College of Dental Medicine, Nova Southeastern University, Fort Lauderdale, Florida

⁵Department of Periodontics and Oral Surgery, University of Ann Arbor, Ann Arbor, Michigan

Correspondence

Yufeng Zhang, Department of Oral Implantology, School and Hospital of Stomatology, Wuhan University, Wuhan 430079, China.
Email: zyf@whu.edu.cn

Funding information

National Natural Science Foundation of China, Grant/Award Numbers: 81771050, 81570954

Abstract

Immune response to implantation materials plays a critical role during early local inflammation and biomaterial-induced regeneration or restoration. A novel platelet concentrate termed i-PRF (injectable platelet-rich fibrin) has recently been developed without any additives by low centrifugation speeds. To date, scientists have investigated the capability of releasing growth factors to improve regeneration but have ignored whether i-PRF can inhibit the inflammatory effect around the wound. The present study investigated the anti-inflammation effects of i-PRF on immune response-related cells, especially macrophages and dendritic cells. We found that i-PRF reduced pro-inflammatory M1 phenotype of macrophages and activated dendritic cells around muscle defect that was injected with bacterial suspension. Moreover, *in vitro* experiments showed similar results. i-PRF deleted inflammatory response caused by lipopolysaccharide to some extent. We determined that TLR4, an activator of inflammatory stimulation and p-p65, a key factor belongs to classical inflammatory related NF- κ B signal pathway, can be inhibited by use of i-PRF. Results indicate the potential anti-inflammatory role of i-PRF during regeneration and restoration.

KEYWORDS

anti-inflammation effects, immune response, i-PRF, regeneration

1 | INTRODUCTION

In regenerative medicine and traumatology, it is vital to regenerate or restore damaged but necessary tissues, such as epithelium, blood vessels and muscles because of an assortment of injury or organ dysfunction (Coury, 2016; Miron et al., 2017a; Zhu et al., 2016). But the induced inflammatory factors surrounding wound retard the operative incision healing after regeneration and restoration (Anaya & Dellinger, 2006). Although the existing majority of tissue engineering scaffolds do not possess anti-inflammatory property by nature, inhibition of inflammation remains essential (Inchingolo et al., 2012).

Recent investigations indicated the importance of regulating the immune response and modulating the immune cells to generate a favorable microenvironment for tissue regeneration and/or restoration (Freytes, Kang, Marcos-Campos, & Vunjak-Novakovic, 2013; Mescher, 2017). Among the several kinds of immune cells, macrophages and dendritic cells (DCs) are particularly non-negligible. Macrophages can be polarized into pro-inflammatory (M1) and anti-inflammatory phenotypes (M2) under different stimulation (Chen et al., 2014; Vogel et al., 2014). M2 macrophages contribute to repair by promoting angiogenesis, tissue remodeling and anti-inflammatory effect (Chen et al., 2017). With regard to DCs (potent antigen-presenting cells), they play a pivotal role in connecting innate and specific immunity (Zhang et al., 2017). Under the condition of bacterial infections, such as osteomyelitis and periodontitis,

Jinglun Zhang and Chengcheng Yin contributed equally to this work.

these two kinds of immune cells were stimulated by lipopolysaccharide (LPS) that induces endotoxin response and nuclear factor-kappa B (NF- κ B) signal pathway activation, which is a symbol of inflammatory response (Boltjes & van Wijk, 2014).

Nowadays, a novel production made from whole blood (WB) without anti-coagulants obtains increasing focus to be further utilized to improve clinical results (Miron et al., 2017b; Miron & Zhang, 2018; Wang, Zhang, Choukroun, Ghanaati, & Miron, 2017). This protocol has been termed platelet-rich fibrin (PRF) (Fujioka-Kobayashi et al., 2017; Miron et al., 2017c; Wang, Zhang, Choukroun, Ghanaati, & Miron, 2018) that contains immune defense cells, which in turn can fight infection (Marrelli & Tatullo, 2013). Furthermore, PRF was originally produced at high centrifugation speeds, thereby permitting a formation of fibrin clot, which act as a 3D scaffold to provide shelter for tissue restoration.

The invention of a disposable formulation of PRF (termed i-PRF) is urgently needed because liquid version can be either utilized alone or associated effortlessly with other biomaterials (Wang et al., 2017). The new one does not contain any anti-coagulants and keep the liquid mobility for approximately 15 min after centrifugation. However, few studies focused on its anti-inflammatory role in wound healing (Miron, Fujioka-Kobayashi, Bishara, et al., 2017c; Miron, Zucchelli, Pikos, et al., 2017a). Therefore, this study aimed to examine the anti-inflammatory effects of i-PRF in vivo and in vitro. The underlying mechanism was also explored.

2 | MATERIALS AND METHODS

2.1 | Preparation of whole blood and i-PRF production

The analyses and reporting on i-PRF in this study followed the previously published on recommendation on standardization of relative centrifugal force values (Ghanaati et al., 2018; Miron, Choukroun, & Ghanaati, 2019; Miron, Fujioka-Kobayashi, Hernandez, et al., 2017b). Whole blood samples were collected from the aortaventralis of eight male Wistar rats (8 weeks of age, 180–200 g weight). All animal settlement and surgical procedures were in the light of the policies of the Ethics Committee for Animal Research, Wuhan University, China (ethical approval number 134/2012). After euthanasia, the animals were placed in a supine position, and a middle abdominal incision was performed at the midpoint of the line between the highest points of the left and right iliac crest and made 4 cm cut. Blunt dissection performed was to allow the direct vision of the aortaventralis for a rapid and precise blood collection.

Special focus was placed on blood collection and i-PRF preparation, as it is important to centrifuge the blood before coagulation starts. 4 ml of whole blood per rat without anticoagulant using a 24-gauge butterfly needle was immediately centrifuged at 700 rpm for 3 min with Choukroun PRF Duo Centrifuge (Process for PRF, Nice, France). RCF expressed in gravitational force (g) was calculated according to the following formula as previously described (Kubesch et al., 2019) $RCF = 1.12 \times \text{Radius} \times (\text{rpm}/1,000)$ (Miron, Zucchelli, Pikos, et al., 2017a).

All of the upper layer was designated the i-PRF. Liquid i-PRF was used for in vivo experiment described as follows. Collected whole blood and i-PRF specimen were transferred to six-well dishes with 5 ml of culture media (DMEM, HyClone, Thermo Fisher Scientific) and processed as further described for in vitro experiments. In each parallel in vitro experiment, the i-PRF used in cell culture was from the same individual.

2.2 | Scanning electron microscopy (SEM)

Samples of coagulated i-PRF were placed into 50 ml centrifuge tubes and quickly washed three times with PBS, fixed 12 hr with 2.5% glutaraldehyde, dehydrated by gradient alcohol, and then sputter-coated with AuPd thin films for SEM (SU7000, Hitachi, Japan) analysis. The morphological evaluation of i-PRF was performed by at 20 kV. SEM images were obtained at magnification ranging from $\times 1,000$ up to $\times 3,000$ at five different field views for each sample.

2.3 | Animal experiments

Twelve adult Wistar rats aged 8 weeks (weighting 250–300 g) were randomly assigned to control group and i-PRF group. Animals were placed under 2.5% isoflurane anesthesia for surgical procedures. Two lower limb gastrocnemius muscle of one rat were made a 5 mm deep cut removing a $10 \times 5 \times 5$ mm piece of the muscle without bleeding. The excised muscles were weighed to confirm the weight to be 15 ± 1.5 mg. Liquid i-PRF well prepared immediately was added into suitable size of gelatin sponge (GS, Xiangen medical technology co., Ltd, China, 20,163,642,299) and transformed into gel state after 30 seconds. Left and right limb from one rat were transplanted with gelatin sponge, *Staphylococcus aureus* (GS + SA) and gelatin sponge, *S. aureus* and i-PRF (GS + SA + i-PRF), respectively.

The pure bacteria in LB were cultured in an incubator at 37°C, obtained a concentration of $2-3 \times 10^9$ CFU ml⁻¹ (OD600 = 0.3 for *S. aureus*). The bacteria solution with a concentration of $2-3 \times 10^7$ ml⁻¹ was prepared for the experiment. In addition, 10ul bacterial suspension was added per defect.

Three days after surgery as reported at study (Miron, Fujioka-Kobayashi, Bishara, et al., 2017c), animals were sacrificed with an overdose of anesthesia. The samples were collected and fixed then dehydrated in a series of alcohol from 30 to 95%, embedded in paraffin wax.

2.4 | Histological staining analysis

The samples were sliced into 5 μ m sections and stained with hematoxylin and eosin (H&E staining).

The antibody used is CD11b (1:150; ABclonal, Cambridge, UK) for immunohistochemical staining. The sections were colored by 3,3-diaminobenzidine tetrahydrochloride (DAB). Then we randomly chose four identical areas in one picture, counted the ratio of CD11b⁺ cells to the total cell number in the selected area by using Image-Pro Plus 6.0 software.

And for immunofluorescent staining, the sections were reacted with primary antibodies iNOS2 (1:200, ABclonal) or CD11c (1:150, CST) and CD86 (1:150, Biolegend). Their secondary antibodies were anti-mouse green fluorescent secondary antibody and anti-rabbit red fluorescent secondary antibody, specifically. The nucleus of cells was stained using DAPI dye in the mounting medium. The images were captured by Olympus DP72 microscope.

2.5 | Cell culture

The murine-derived macrophages RAW264.7 and dendritic cell line DC2.4 (DCs), purchased from Cbioer Biotechnology Co., Ltd, were used in this study. Cells were cultured in 10-cm culture dishes containing DMEM supplemented with 10% fetal bovine serum (FBS; Gibco, Life Technologies Corporation) at 37°C in a humidified 5% CO₂ incubator.

Platelet concentrates i-PRF were cultured for three days in cell incubator and thereafter i-PRF conditioned media was collected as 20% of the total volume as previously described (Wang et al., 2017). Cells were seeded with 20% conditioned media from i-PRF at a density of 100,000 cells in six-well plates stimulated by lipopolysaccharide (LPS) at dose of 100 ng/ml. After 24 hr stimulating, RNA and protein were collected as follows.

2.6 | RNA extraction and RT-qPCR

Total RNA was extracted by Trizol reagent (TriPure Isolation Reagent, Roche Applied Science, Germany) and complementary DNA was synthesized from 1 µg of total RNA using PrimeScript RT-PCR Kit (TaKaRa, Japan) referred to the manufacturer's instruction. RT-qPCR was performed using Prime-Script RT-PCR Kit (TaKaRa, Japan). The primer sequences of target genes are listed in Table 1. Every marker was tested by five replicates.

2.7 | Protein extraction and western blot

RIPA lysate (containing 1 mM PMSF) was used to extract the total protein. Proteins were separated by SDS-PAGE then transferred to nitrocellulose membranes. The membranes were blocked using 5% non-fat milk for 1 hr at room temperature and incubated with primary antibodies against GAPDH (1:5000, proteintech, China.), TLR4 (1:1000, ABclonal), iNOS2 (1:1000, Sant Cruz), p-65 (1:1000, CST), TRAF6 (1:1000, Boster, China), p-p65 (1:1000, CST), and ARG1 (1:1000, ABclonal) at 4°C overnight, followed by secondary antibodies (Biosharp) for 1 hr at room temperature. Protein bands were visualized using WesternBright ECL HRP substrate Kit (Advansta). Western blot was conducted by three replicates and relative intensity was calculated by Image-Pro Plus 6.0 software.

2.8 | Statistical analysis

The statistical analyses were finished by the GraphPad Prism software 7.0 (GraphPad, San Diego, CA). Non-parametric test and Students'

TABLE 1 Primers used for real-time PCR

Gene primers	(F, forward; R, reverse)
TNF- α	F: 5'-GACGTGGAAGTGGCAGAAGAG-3' R: 5'-TTGGTGGTTTGTGAGTGTGAG-3'
GAPDH	F: 5'-TGACCACAGTCCATGCCATC-3' R: 5'-GACGGACACATTGGGGGTAG-3'
IL-6	F: 5'-CCAAGAGGTGAGTGCTTCCC-3' R: 5'-CTGTTGTTTCAGACTCTCTCCCT-3'
iNOS2	F: 5'-GTTCTCAGCCCAACAATACAAGA-3' R: 5'-GTGGACGGTTCGATGTAC-3'
CD206	F: 5'-CTCTGTTTCAGCTATTGGACGC-3' R: 5'-CGGAATTTCTGGATTAGCTTC-3'
CD86	F: 5'-ATGGACCCAGATGCACCA-3' R: 5'-CTGTGCCAAATAGTGCTCG-3'
TLR4	F: 5'-ACTTGATACTGACAGGAAACCC-3' R: 5'-TTCCCTGAAAGGCTTGGTCT-3'
TRAF6	F: 5'-CGCTGTGAAGTCTCTACCCG-3' R: 5'-GTACATGGACGCTACACCC-3'
MHCII	F: 5'-CGAAACTGAAAACGGCAAGACG-3' R: 5'-AGGCAGCTACCCTCCGATT-3'

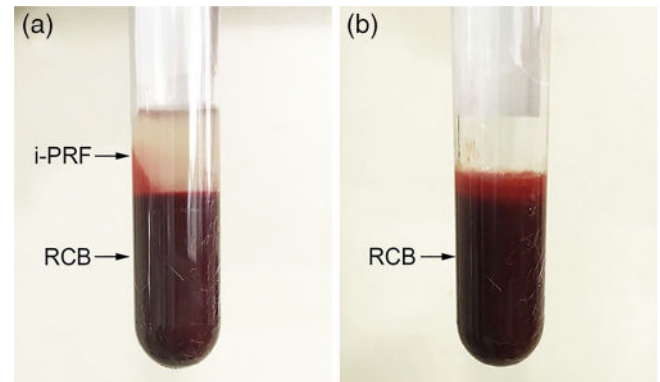


FIGURE 1 i-PRF characterization. (a) The morphology of i-PRF after centrifugation at utilizing non-glass centrifugation tubes. (b) Remaining of red corpuscles base and platelet plasma after transfer of i-PRF. RCB, red corpuscles base

t-test were used to analysis differences. *p*-values less than .05 were considered as statistical significance.

3 | RESULTS

3.1 | I-PRF characterization

After preparation of i-PRF, as shown in Figure. 1, we examined the surface morphology of i-PRF (Figure. 2) by scanning electron microscopy (SEM). Images revealed the amounts of activated platelets, lymphocytes, and red blood cells embedded in an anfractuous three-dimensional fibrin network formed during the i-PRF production procedure.

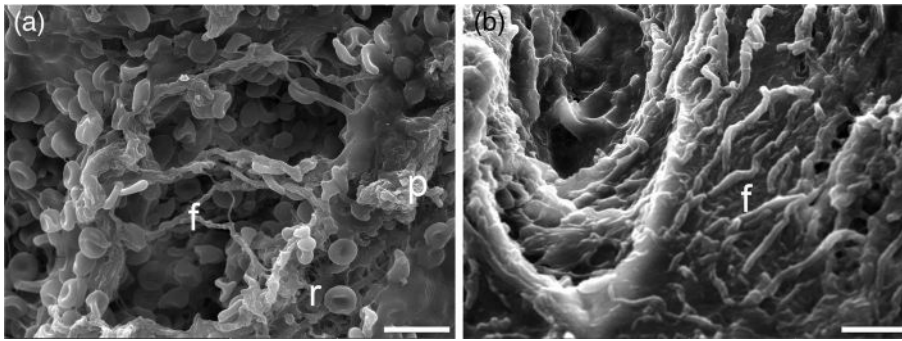


FIGURE 2 The surface (a) and cross-section microstructures (b) of the i-PRF. f, fibrin; p, platelet aggregates; r, red blood cell. Scale bar = 10 μm

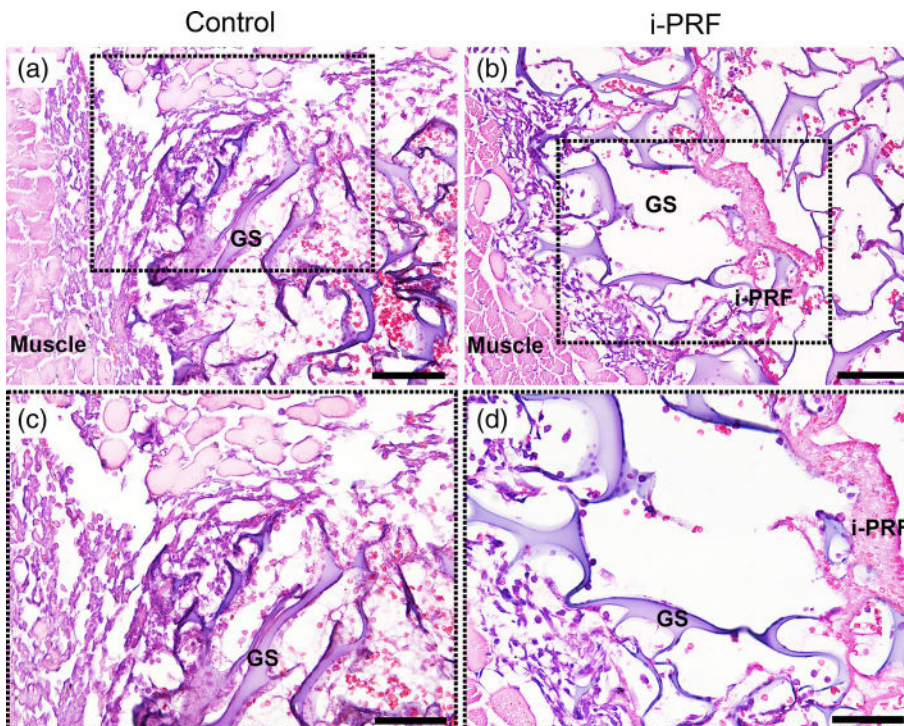


FIGURE 3 H&E staining sections of muscle defect from control (a, c) and i-PRF groups (b, d). Less inflammatory cells were surrounded around defects in i-PRF group. Abbreviation: GS, gelatin sponge. Scale bar in a, b = 50 μm ; c, d = 20 μm

3.2 | Rat muscle defects filled with or without i-PRF

To study the anti-inflammatory effects of i-PRF *in vivo*, we firstly made a rat muscle defect model to provide space for material transplanting. *S. aureus* was used to induce a local inflammatory response. Histological appearance of hematoxylin and eosin staining of the defects at 3 days after surgery (Figure. 3) showed that muscle tissues around the injury were filled with or without i-PRF. And there was less inflammatory cells infiltration in i-PRF groups.

3.3 | Immunohistochemical staining of rat muscle defect filled with or without i-PRF

Samples were then immunohistochemically stained CD11b to observe overall innate immune cells (Figure 4). Adding i-PRF dramatically decreased the amount of local innate immune cells. This condition is conducive to wound healing, indicating that i-PRF would affect these innate immune cells to play a pivotally anti-inflammatory role.

3.4 | Effects of i-PRF on the polarization of macrophages

We processed the immunofluorescent staining of tissue samples to further investigate one of the predominant innate immune cells as follows. Macrophages were stained with biomarkers induced with nitric oxide synthase 2 (iNOS2), as exhibited in Figure 5a,b. Meanwhile, we stimulated murine-derived macrophage cell line RAW 264.7 cells with LPS at dose of 100 ng/ml and then compared the anti-inflammatory consequence between the treated WB and the i-PRF groups. To clarify the expression of polarization properties, real-time quantitative polymerase chain reaction (RT-qPCR) was performed (Figure 5c). Among the pro-inflammatory M1 markers, TNF α and IL-6 expressions decreased due to suppression, whereas ARG1 and CD206 expressions increased because of activation with i-PRF compared with WB. What's more, i-PRF inhibited p65 phosphorylation and expression of Toll-like receptor 4 (TLR4), as revealed by Western Blot analysis (Figure 5d,e). iNOS2 and ARG1 expressions also changed correspondingly.

FIGURE 4 The expressions of CD11b in tissues from control (a, c) and i-PRF groups (b, d). (e) Quantification of the immunohistochemical staining was calculated by the percentage of CD11b positive cells in all cells in the area of the same size. **** $p < .0001$. Error bars indicate SD. Scale bar in a, b = 20 μm , c, d = 10 μm

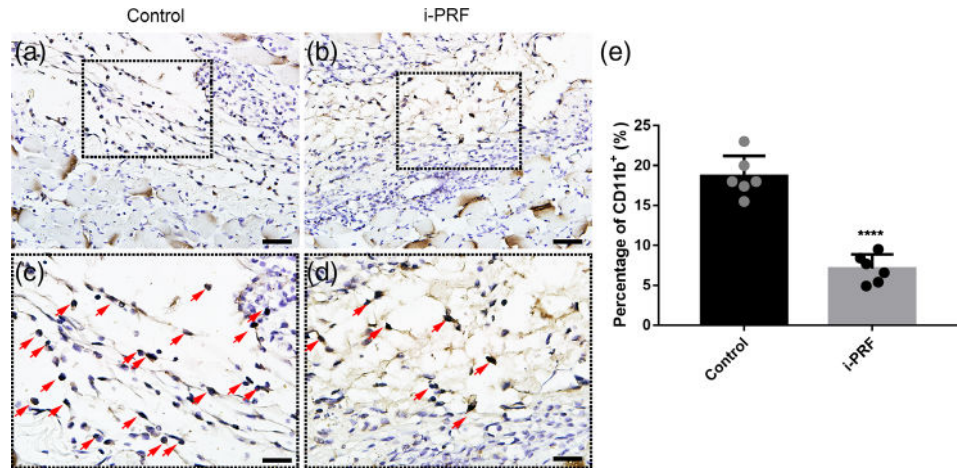
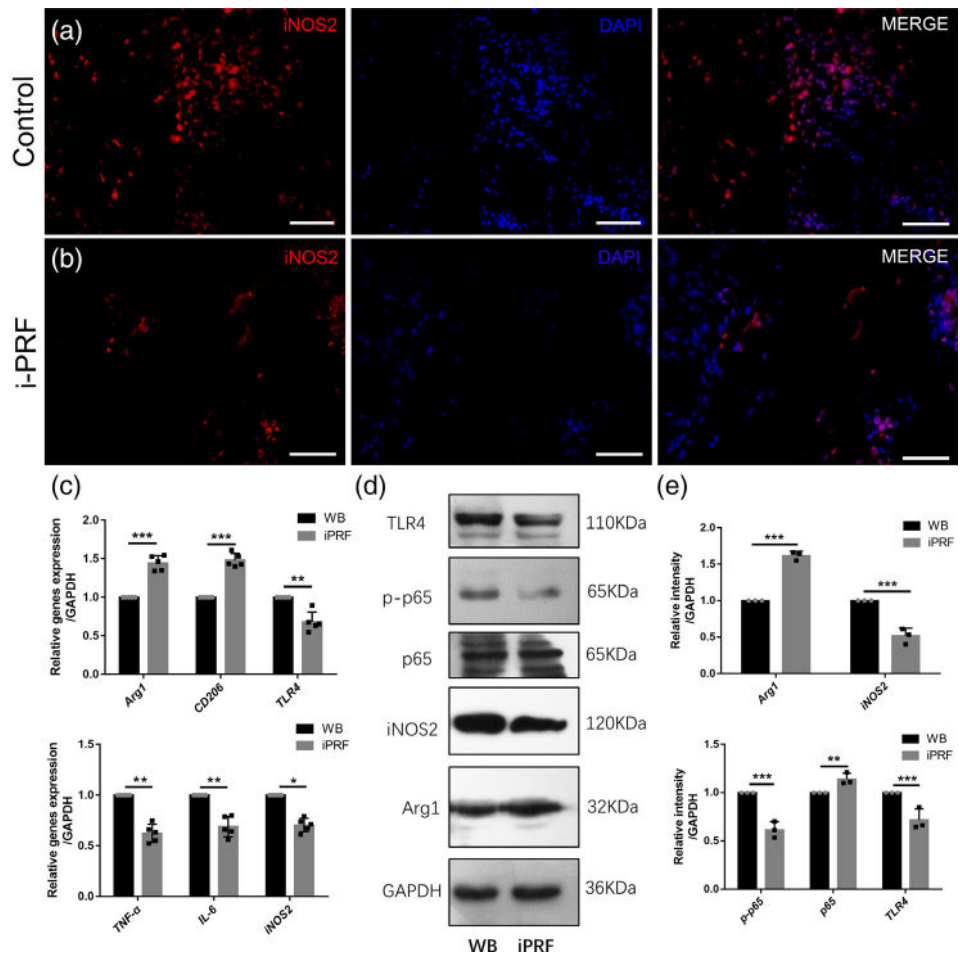


FIGURE 5 Effects of i-PRF on the polarization of macrophages. (a, b) Sections of immunofluorescence with antibodies against iNOS2. Scale bar = 20 μm . (c) Relative expressions of polarization related genes and TLR4 in RAW264.7. (d) Immunoblotting (e) relative intensity of NF- κB signaling pathway and polarization related markers of RAW264.7 stimulated by the WB or i-PRF in the presence of LPS. * $p < .05$, ** $p < .005$, *** $p < .0005$. Error bars indicate SD. LPS, lipopolysaccharide; WB, whole blood



3.5 | Effects of i-PRF on the maturation of dendritic cell

To further determine the mechanism of i-PRF affects DCs, histopathological specimens immunofluorescent stained with CD11c and CD86, as exhibited in Figure 6a,b. Moreover, we stimulated murine-derived DC line DC2.4 cells with LPS at similar dose and treated them with WB or i-PRF. To characterize the DC activation, mRNA levels of related genes CD86 and major histocompatibility complex II (MHC II) were evaluated by RT-qPCR (Figure 6c). Notably, i-PRF obviously

downregulated two genes expression levels, as shown in Figure 6. Meanwhile, i-PRF reduced protein expression of phosphorylated p65, TLR4 and TNF receptor-associated factor 6 (TRAF6) via Western Blot analysis. (Figure 6d,e).

4 | DISCUSSION

i-PRF has been developed for several years, but few studies have focused on i-PRF's anti-inflammatory role in wound healing

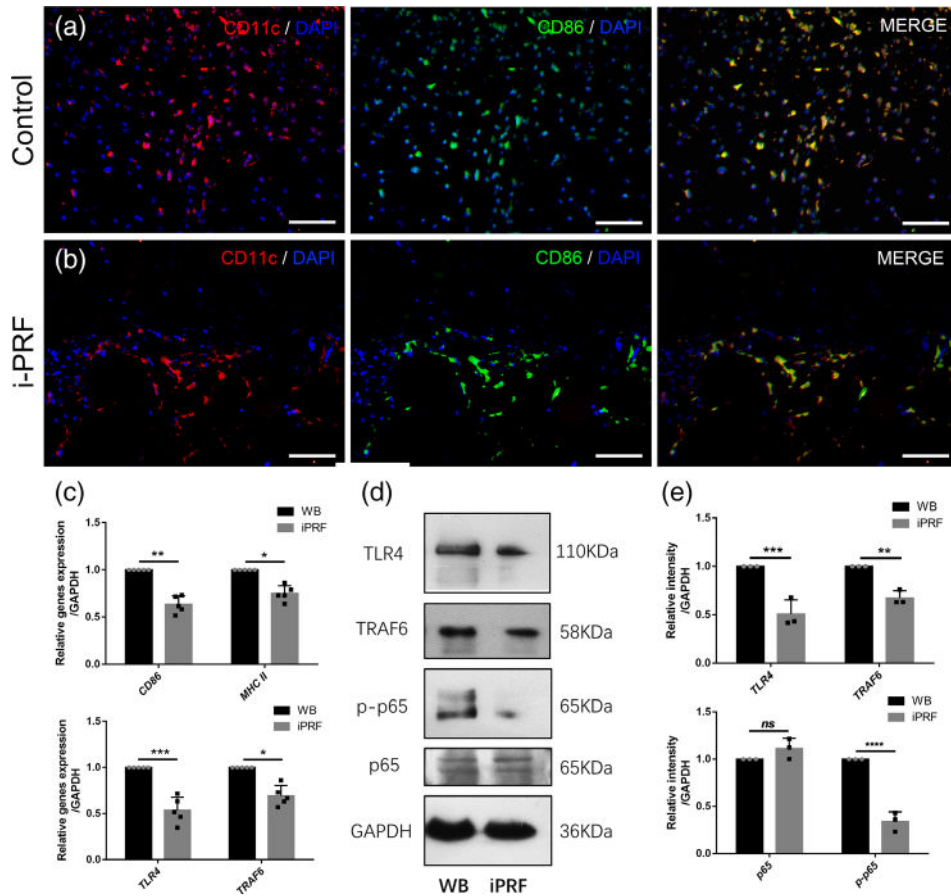


FIGURE 6 Effects of i-PRF on the maturation of dendritic cells. (a, b) Sections of immunofluorescence with antibodies against CD11c and CD86. Scale bar = 20 μm. (c) Relative expressions of maturation related and inflammatory related genes in DC2.4. (d) Immunoblotting and (e) relative intensity of NF-κB signaling pathway and maturation related markers of DC2.4 stimulated by the presence of LPS. * $p < .05$, ** $p < .005$, *** $p < .0005$, **** $p < .0001$, ns indicates no significant difference. Error bars indicate SD. LPS, lipopolysaccharide; WB, whole blood

(Miron, Fujioka-Kobayashi, Hernandez, et al., 2017b). Thus, the present study aimed to (a) investigate and compare the influence of i-PRF in liquid formulation versus WB on tissue wound and (b) investigate its underlying mechanism. To the greatest of the authors' view, this work is the first study to investigate the anti-inflammatory influence of i-PRF.

A numbers of xenograft biomaterials are stereotyped to be commercialized including porcine and bovine-derived (Coury, 2016; Zhu et al., 2016). The use of PRF in regenerative medicine has become increasingly popular because of its low-cost and enhanced curative effect (Kobayashi et al., 2016; Miron, Fujioka-Kobayashi, Bishara, et al., 2017c; Miron, Zucchelli, Pikos, et al., 2017a). Moreover, PRF acts as an entirely autologous biomaterial and thus does not elicit a foreign body reaction. After centrifugation at 700 rpm for 3 min, the faint yellow upper layer is i-PRF, and substratum is red corpuscles base.

A major research development was the formulation of a liquid version of PRF, termed injectable-PRF, or i-PRF. This version was intended to advance biomaterial blending with platelet concentrates, and to form a fibrin network following coating (Miron, Fujioka-Kobayashi, Hernandez, et al., 2017b). We previously demonstrated by decreasing centrifugation speed and time, growth factor release and cell activity increased (Abd El Raouf et al., 2019; Varela et al., 2019). The immune response to biomaterials possesses a vital role in influencing either an inflammatory reaction or biomaterial-mediated tissue regeneration (Franz, Rammelt, Scharnweber, & Simon, 2011). However, studies on immune cell responses to such

biomaterials have been minimal. In reality, the immune system and regeneration or trauma restoration exhibit interaction especially when foreign biomaterials are transplanted into host tissues (Giridharan & Srinivasan, 2018; Liu et al., 2019a). Because we still do not know the underlying mechanism about anti-inflammatory effect of i-PRF on main innate immune cells, we chose whole blood as a control. In this study, we found that i-PRF has greater anti-inflammatory response than WB. In future research, we hope to determine whether i-PRF has distinct anti-inflammatory ingredients compared to other blood products.

NF-κB signaling is important in innate immune responses mediated by innate immune cells, including DCs and macrophages (Vogel et al., 2014; Zhang et al., 2017). DCs and macrophages express toll-like receptors (TLRs) to activate NF-κB, producing pro-inflammatory cytokines, including IL-1β, IL-6, and TNF-α, during microbial infection (Agoro, Taleb, Quesniaux, & Mura, 2018; Basak, Behar, & Hoffmann, 2012; Bista et al., 2010). Macrophages and DCs are important immune cells. Anti-inflammatory M2-polarized macrophage phenotype-associated cytokines (ARG1, IL-10, TGF-β, and CD206) are increased in i-PRF. DC function depends mainly on degree of maturation (Boltjes & van Wijk, 2014). DC maturation is accompanied by the upregulation of co-stimulatory molecules including CD86, CD80, MHC II, and IL-12, which also can be down-regulated by treating with i-PRF. Furthermore, in the present study, we discovered that TLR4, TRAF6 and phosphorylation of p65, a key factor of NF-κB signal pathway, were markedly restricted by i-PRF (Bista et al., 2010). Since the primary macrophages of different individuals differed,

we did not extract primary cells. Although many literatures have reported the use of i-PRF to treat cells of heterogeneous origin (Dai et al., 2019; do Lago, Ferreira, Garcia Jr., Okamoto, & Mariano, 2019; Kargarpour et al., 2019; Liu et al., 2019b), this is a limitation of current research. For example, without using primary cells, it may not be possible to accurately simulate the immune response in the body. In addition, Overall, i-PRF can restrain the activation of DC and pro-inflammatory M1 phenotype polarization but promote anti-inflammatory M2 swift.

The NF- κ B signaling pathway can be activated TLRs, and then, TNF receptor-associated factor 6 (TRAF6) activates the inhibitor of κ B kinase (IKK), thereby leading to phosphorylation and ubiquitination-proteasome-dependent degradation of the inhibitor of NF- κ B (I κ B α) (Basak et al., 2012). Subsequently, I κ B-released p65 and p50 form a complex and translocate into the nucleus upon initiation of targeted gene transcription (Tian et al., 2017). During this process, p65 is phosphorylated by IKK (Liu et al., 2017). As reported, several diseases were related to no normal phosphorylation of p65 (p-p65) (Basak et al., 2012; Bista et al., 2010; Liu et al., 2017; Liu, Zhou, et al., 2019a). Therefore, we concentrated on whether or not i-PRF has influence on phosphorylation of p65 or not. Obviously, i-PRF inhibited not only the p-p65 expression but also its initiator TLR4. From the perspective of regeneration, it has shown the benefits of controlled inflammation in regular tissue healing and recovery. However, several factors, for example, severity and lasting time of inflammatory should be considered. In current study, we focused on the anti-inflammatory effect of i-PRF on innate immune cells. Moreover, the infection was not thoroughly inhibited by i-PRF. Further investigations about the dosage of i-PRF and the degree of inflammation control on the effects of regeneration should be done in the future.

Collectively, i-PRF affected the response of immune cells in vivo or in vitro, and i-PRF suppressed DC maturation and macrophage M1 polarization by altering the expression of costimulatory molecules and inflammatory cytokines. Therefore, i-PRF addition under the condition of regenerative, trauma surgery or inflammatory disease can alleviate the immune response, thereby favoring restoration and healing, and may be a suitable strategy to ease patients' pain and meet clinical needs. Meanwhile, further research is necessary for detailed constituents of i-PRF, to further evaluate its comprehensive potential. This study is a first to characterize the influence of i-PRF on immune response.

ORCID

Jinglun Zhang  <https://orcid.org/0000-0002-1998-8851>

Qin Zhao  <https://orcid.org/0000-0003-4223-9522>

Yufeng Zhang  <https://orcid.org/0000-0001-8702-5291>

REFERENCES

- Abd El Raouf, M., Wang, X., Miusi, S., Chai, J., Mohamed AbdEl-Aal, A. B., Nefissa Helmy, M. M., et al. (2019). Injectable-platelet rich fibrin using the low speed centrifugation concept improves cartilage regeneration when compared to platelet-rich plasma. *Platelets*, 30(2), 213–221.
- Agoro, R., Taleb, M., Quesniaux, V. F. J., & Mura, C. (2018). Cell iron status influences macrophage polarization. *PLoS One*, 13(5), e0196921.
- Anaya, D. A., & Dellinger, E. P. (2006). The obese surgical patient: A susceptible host for infection. *Surgical Infections*, 7(5), 473–480.
- Basak, S., Behar, M., & Hoffmann, A. (2012). Lessons from mathematically modeling the NF-kappaB pathway. *Immunological Reviews*, 246(1), 221–238.
- Bista, P., Zeng, W., Ryan, S., Bailly, V., Browning, J. L., & Lukashev, M. E. (2010). TRAF3 controls activation of the canonical and alternative NFkappaB by the lymphotoxin beta receptor. *The Journal of Biological Chemistry*, 285(17), 12971–12978.
- Boltjes, A., & van Wijk, F. (2014). Human dendritic cell functional specialization in steady-state and inflammation. *Frontiers in Immunology*, 5, 131.
- Chen, Z., Ni, S., Han, S., Crawford, R., Lu, S., Wei, F., ... Xiao, Y. (2017). Nanoporous microstructures mediate osteogenesis by modulating the osteo-immune response of macrophages. *Nanoscale*, 9(2), 706–718.
- Chen, Z., Wu, C., Gu, W., Klein, T., Crawford, R., & Xiao, Y. (2014). Osteogenic differentiation of bone marrow MSCs by beta-tricalcium phosphate stimulating macrophages via BMP2 signalling pathway. *Biomaterials*, 35(5), 1507–1518.
- Coury, A. J. (2016). Expediting the transition from replacement medicine to tissue engineering. *Regenerative Biomaterials*, 3(2), 111–113.
- Dai, T. Q., Zhang, L. L., An, Y., Xu, F. F., An, R., Xu, H. Y., ... Liu, B. (2019). In vitro transdifferentiation of adipose tissue-derived stem cells into salivary gland acinar-like cells. *American Journal of Translational Research*, 11(5), 2908–2924.
- do Lago, E. S., Ferreira, S., Garcia, I. R., Jr., Okamoto, R., & Mariano, R. C. (2019). Improvement of bone repair with I-PRF and bovine bone in calvaria of rats. Histometric and immunohistochemical study. *Clinical Oral Investigations*. <https://doi.org/10.1007/s00784-019-03018-4>.
- Franz, S., Rammelt, S., Scharnweber, D., & Simon, J. C. (2011). Immune responses to implants - a review of the implications for the design of immunomodulatory biomaterials. *Biomaterials*, 32(28), 6692–6709.
- Freytes, D. O., Kang, J. W., Marcos-Campos, I., & Vunjak-Novakovic, G. (2013). Macrophages modulate the viability and growth of human mesenchymal stem cells. *Journal of Cellular Biochemistry*, 114(1), 220–229.
- Fujioka-Kobayashi, M., Miron, R. J., Hernandez, M., Kandalam, U., Zhang, Y., & Choukroun, J. (2017). Optimized platelet-rich fibrin with the low-speed concept: Growth factor release, biocompatibility, and cellular response. *Journal of Periodontology*, 88(1), 112–121.
- Ghanaati, S., Al-Maawi, S., Herrera-Vizcaino, C., Alves, G. G., Calasans-Maia, M. D., Sader, R., ... Mourao, C. (2018). A proof of the low speed centrifugation concept in rodents: New perspectives for in vivo research. *Tissue Engineering. Part C, Methods*, 24(11), 659–670.
- Giridharan, S., & Srinivasan, M. (2018). Mechanisms of NF-kappaB p65 and strategies for therapeutic manipulation. *Journal of Inflammation Research*, 11, 407–419.
- Inchingolo, F., Tatullo, M., Marrelli, M., Inchingolo, A. M., Inchingolo, A. D., Dipalma, G., et al. (2012). Regenerative surgery performed with platelet-rich plasma used in sinus lift elevation before dental implant surgery: An useful aid in healing and regeneration of bone tissue. *European Review for Medical and Pharmacological Sciences*, 16(9), 1222–1226.
- Kargarpour, Z., Nasirzade, J., Strauss, F. J., Summa, F. D., Hasannia, S., Muller, H. D., & Gruber, R. (2019). Platelet-rich fibrin suppresses in vitro osteoclastogenesis. *Journal of Periodontology*. <https://doi.org/10.1002/JPER.19-0109>.
- Kobayashi, E., Fluckiger, L., Fujioka-Kobayashi, M., Sawada, K., Sculean, A., Schaller, B., & Miron, R. J. (2016). Comparative release of growth factors from PRP, PRF, and advanced-PRF. *Clinical Oral Investigations*, 20(9), 2353–2360.
- Kubesch, A., Barbeck, M., Al-Maawi, S., Orłowska, A., Booms, P. F., Sader, R. A., ... Ghanaati, S. (2019). A low-speed centrifugation concept leads to cell accumulation and vascularization of solid platelet-rich fibrin: An experimental study in vivo. *Platelets*, 30(3), 329–340.

- Liu, C., Zhou, Y., Li, M., Wang, Y., Yang, L., Yang, S., et al. (2019a). Absence of GdX/UBL4A protects against inflammatory diseases by regulating NF-small ka, CyrillicB signaling in macrophages and dendritic cells. *Theranostics*, 9(5), 1369–1384.
- Liu, Y., Fang, S., Li, X., Feng, J., Du, J., Guo, L., et al. (2017). Aspirin inhibits LPS-induced macrophage activation via the NF-kappaB pathway. *Scientific Reports*, 7(1), 11549.
- Liu, Z., Jin, H., Xie, Q., Jiang, Z., Guo, S., Li, Y., & Zhang, B. (2019b). Controlled release strategies for the combination of fresh and lyophilized platelet-rich fibrin on bone tissue regeneration. *BioMed Research International*, 2019, 4923767.
- Marrelli, M., & Tatullo, M. (2013). Influence of PRF in the healing of bone and gingival tissues. Clinical and histological evaluations. *European Review for Medical and Pharmacological Sciences*, 17(14), 1958–1962.
- Mescher, A. L. (2017). Macrophages and fibroblasts during inflammation and tissue repair in models of organ regeneration. *Regeneration*, 4(2), 39–53.
- Miron, R. J., Choukroun, J., & Ghanaati, S. (2019). Reply from authors: RE: Optimized platelet-rich fibrin with the low-speed concept: Growth factor release, biocompatibility, and cellular response: Necessity for standardization of relative centrifugal force values in studies on platelet-rich fibrin. *Journal of Periodontology*, 90(2), 122–125.
- Miron, R. J., Fujioka-Kobayashi, M., Bishara, M., Zhang, Y., Hernandez, M., & Choukroun, J. (2017c). Platelet-rich fibrin and soft tissue wound healing: A systematic review. *Tissue Engineering. Part B, Reviews*, 23(1), 83–99.
- Miron, R. J., Fujioka-Kobayashi, M., Hernandez, M., Kandam, U., Zhang, Y., Ghanaati, S., & Choukroun, J. (2017b). Injectable platelet rich fibrin (i-PRF): Opportunities in regenerative dentistry? *Clinical Oral Investigations*, 21(8), 2619–2627.
- Miron, R. J., & Zhang, Y. (2018). Autologous liquid platelet rich fibrin: A novel drug delivery system. *Acta Biomaterialia*, 75, 35–51.
- Miron, R. J., Zucchelli, G., Pikos, M. A., Salama, M., Lee, S., Guillemette, V., et al. (2017a). Use of platelet-rich fibrin in regenerative dentistry: A systematic review. *Clinical Oral Investigations*, 21(6), 1913–1927.
- Tian, L., Li, W., Yang, L., Chang, N., Fan, X., Ji, X., ... Li, L. (2017). Cannabinoid receptor 1 participates in liver inflammation by promoting M1 macrophage polarization via RhoA/NF-kappaB p65 and ERK1/2 pathways, respectively, in mouse liver Fibrogenesis. *Frontiers in Immunology*, 8, 1214.
- Varela, H. A., Souza, J. C. M., Nascimento, R. M., Araujo, R. F., Jr., Vasconcelos, R. C., Cavalcante, R. S., ... Araujo, A. A. (2019). Injectable platelet rich fibrin: Cell content, morphological, and protein characterization. *Clinical Oral Investigations*, 23(3), 1309–1318.
- Vogel, D. Y., Glim, J. E., Stavenuiter, A. W., Breur, M., Heijnen, P., Amor, S., ... Beelen, R. H. (2014). Human macrophage polarization in vitro: Maturation and activation methods compared. *Immunobiology*, 219(9), 695–703.
- Wang, X., Zhang, Y., Choukroun, J., Ghanaati, S., & Miron, R. J. (2017). Behavior of gingival fibroblasts on titanium implant surfaces in combination with either injectable-PRF or PRP. *International Journal of Molecular Sciences*, 18(2), 331.
- Wang, X., Zhang, Y., Choukroun, J., Ghanaati, S., & Miron, R. J. (2018). Effects of an injectable platelet-rich fibrin on osteoblast behavior and bone tissue formation in comparison to platelet-rich plasma. *Platelets*, 29(1), 48–55.
- Zhang, L., Ke, J., Wang, Y., Yang, S., Miron, R. J., & Zhang, Y. (2017). An in vitro investigation of the marked impact of dendritic cell interactions with bone grafts. *Journal of Biomedical Materials Research. Part A*, 105(6), 1703–1711.
- Zhu, W., Ma, X., Gou, M., Mei, D., Zhang, K., & Chen, S. (2016). 3D printing of functional biomaterials for tissue engineering. *Current Opinion in Biotechnology*, 40, 103–112.

How to cite this article: Zhang J, Yin C, Zhao Q, et al. Anti-inflammation effects of injectable platelet-rich fibrin via macrophages and dendritic cells. *J Biomed Mater Res*. 2019; 1–8. <https://doi.org/10.1002/jbm.a.36792>